

Structural, elastic, thermal, and electronic response of small-molecule-loaded metal organic framework materials

— Supplementary Information —

Pieremanuele Canepa,^{†,§} Kui Tan,[‡] Yingjie Du,[¶] Hongbing Lu,[¶] Yves J. Chabal,[‡]
and T. Thonhauser^{*,†}

*Department of Physics, Wake Forest University, Winston-Salem, NC 27109, USA,
Department of Materials Science and Engineering, University of Texas at Dallas, TX
75080, USA, and Department of Mechanical Engineering, University of Texas at Dallas,
TX 75080, USA*

E-mail: thonhauser@wfu.edu

1 Theoretical quantities

Starting from the complete vibrational spectrum of the MOF, we can calculate macroscopic properties such as the specific heat at constant volume, C_v , and the thermal expansion, α . In Eq. (1) we connect C_v , computed from Einstein's model, with the vibrational frequencies of the MOF:

$$C_v = 3k_b \sum_i \left(\frac{\hbar\omega_i}{2k_bT} \right)^2 \sinh^{-2} \left(\frac{\hbar\omega_i}{2k_bT} \right). \quad (1)$$

Here, k_b is Boltzmann's constant, T the temperature, and ω_i the i^{th} IR/Raman frequency. Note that the summation in Eq. (1) runs over *all* vibrations of the system. However, due to the large dimensions of the MOF-74-Zn cell, it

is sufficient to limit the evaluation of C_v and α to the optical phonon branch at the Γ -point. To find the phonons at Γ , the dynamical matrix was computed, using a three-point formula with a well-converged displacement of 0.01 Å.

C_v of Eq. (1) is the main ingredient for computing the thermal expansion α :

$$\alpha = \frac{\gamma C_v}{3B}, \quad (2)$$

where B is the bulk modulus of the material, and γ is related to the Grüneisen parameter. The latter is the negative logarithmic derivative of the normal-mode frequency with respect to a change in volume, i.e. $-\partial(\ln \omega_i)/\partial(\ln V)$.¹ The *ab initio* calculation of γ for the present MOF is computationally prohibitively expensive; we thus estimate it using the Universal Force Field² as implemented in GULP,³⁻⁵ assigning the atomic charges according to previous studies on MOF-74-Zn.⁶ Note that the computation of γ does not require highly accurate phonon frequencies, making its evaluation more feasible even with classical potentials.

The elastic response of MOF-74-Zn upon molecular adsorption was measured by monitoring the variation of the elastic tensor, as can

*To whom correspondence should be addressed

[†]Department of Physics, Wake Forest University, Winston-Salem, NC 27109, USA

[‡]Department of Materials Science and Engineering, University of Texas at Dallas, TX 75080, USA

[¶]Department of Mechanical Engineering, University of Texas at Dallas, TX 75080, USA

[§]Current address: Department of Materials Science and Engineering, Massachusetts Institute of Technology, Cambridge, MA 02139, USA

be seen from the stress-strain relationship according to the Voight notation of Eq. (3):

$$\sigma_{ij} = C_{ij}\epsilon_{ij} . \quad (3)$$

Here, σ_{ij} are the components of the second-rank stress tensor, C_{ij} are the elastic constants, and ϵ_i is the vector defining the strain directions. By knowing the tensor C and its inverse $S = C^{-1}$ (the compliance tensor) one can calculate the corresponding bulk (B), shear (G), and Young's (Y) moduli via the Voight-Reuss-Hill approach.⁷ Voight-Reuss moduli define an upper and lower bound of these elastic properties and they are averaged by the Hill definition.⁷ Poisson's ratios, ν , is another macroscopic property that measures the ratio of lateral to longitudinal strain under a uniform, uniaxial stress, as defined by Eq. (4),

$$\nu_i(j) = -S_{ij}Y_j , \quad (4)$$

where S_{ij} are the elements of the compliance tensor, while Y_j is the Young's modulus along the j direction. The longitudinal (v_l), transversal (v_t), and mean (v_m) sound velocities are related to the bulk and shear moduli:

$$v_l = \left(\frac{3B + 4G}{3\rho} \right)^{\frac{1}{2}} , \quad (5)$$

$$v_t = \left(\frac{G}{\rho} \right)^{\frac{1}{2}} , \quad (6)$$

$$v_m = \left[\frac{1}{3} \left(\frac{2}{v_t^3} + \frac{1}{v_l^3} \right) \right]^{-\frac{1}{3}} , \quad (7)$$

where ρ is the density of the material. Finally, v_m is important for the calculation of the Debye temperature, Θ_D , which is related to C_v from Eq. (1), and thus to the rigidity of the MOF:

$$\Theta_D = \frac{h}{k_b} \left(\frac{3n N_A}{4\pi V} \right)^{\frac{1}{3}} v_m . \quad (8)$$

Here, h is Planck's constants, N_A Avogadro's number, n the number of atoms, and V the volume of the MOF.

The elastic tensors, from which the other properties discussed above are determined, are calculated using a central-difference method.

To this end, we used a step size of 0.01 Å and applied six finite distortions to the lattice, allowing us to find the elastic constants from the strain-stress relationship in Eq. (3).

2 Nano-indentation and Oliver and Pharr's method

Over the past two decades, nano-indentation has been used for the measurement of mechanical properties such as elasticity and viscoelasticity.^{8,9} The instrumented nano-indenter is widely accepted as a standardized testing method for characterization of elastic-plastic materials. The resolution can reach a fraction of a nm in displacement and μN in load. As a result, the nano-indentation technique is widely used to extract mechanical properties of materials with very small volumes, such as thin foils, wires, and micro-electromechanical systems.

During the experiment, the vertically applied load on the indenter tip is increased until it reaches a user-defined value and its displacement is measured continuously. Illustrations of the indentation and the typical load vs. displacement curve are shown in Fig. S1 and Fig. S2. An optical microscope image of the crystal we used for our experiments is depicted in Fig. S3.

The most widely used method to extract Young's modulus from a load vs. displacement curve obtained through nano-indentation was proposed by Oliver and Pharr in 1992.⁸ As shown in Fig. S1, the maximum displacement is divided into two parts, the sink-in displacement h_s and contact displacement h_c . The value of h_s is given by Eq. (9) as

$$h_s = \varepsilon \frac{P_{max}}{S} , \quad (9)$$

where P_{max} is the maximum indentation force and ε is a constant, which depends on the geometry of the indenter; for a Berkovich indenter tip, ε is 0.72. The contact stiffness, S , is provided by the slope of the initial unloading curve.

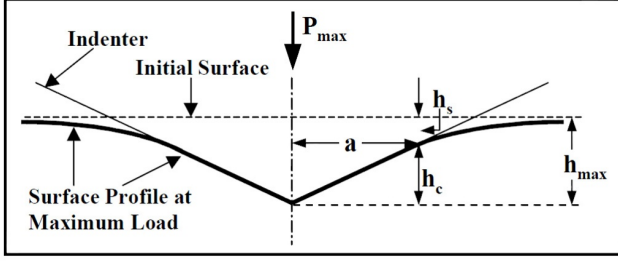


Figure S1: Illustration of the indentation geometry at maximum load.

The contact displacement then becomes

$$h_c = h_{max} - \varepsilon \frac{P_{max}}{S}. \quad (10)$$

Based on the contact mechanics analysis of nano-indentation, the hardness (H) is obtained using Eq. (11)

$$H = \frac{P_{max}}{A_c}, \quad (11)$$

where for a Berkovich tip the contact area is $A_c = 24.5 h_c^2$. Measurement of the elastic modulus follows from its relationship to the contact area and the measured unloading stiffness through the relation⁸

$$S = \frac{2}{\sqrt{2\pi}} Y_r \sqrt{A_c}, \quad (12)$$

where Y_r is the reduced modulus defined by

$$\frac{1}{Y_r} = \frac{1 - \nu_s^2}{Y_s} + \frac{1 - \nu_i^2}{Y_i}, \quad (13)$$

and Y_s and ν_s are the Young's modulus and Poisson's ratio of the specimen, while Y_i and ν_i are the corresponding values of the diamond indenter tip. Equations (12) and (13) along with the known values of the unloading-curve slope, modulus, and Poisson's ratio values for the indenter tip can be used to determine the elastic modulus for a specimen corresponding to its Poisson's ratio.

3 IR measurements

After water adsorption under 8 Torr H_2O vapor, the MOFs phonon modes such as the benzene

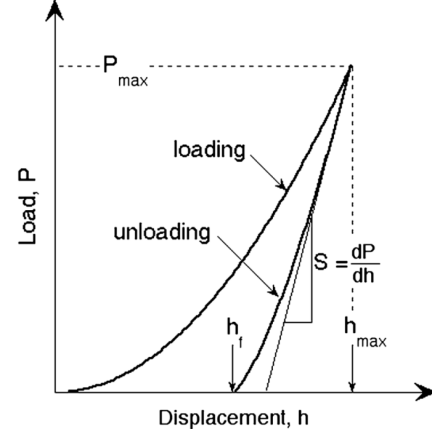


Figure S2: A typical load vs. displacement curve for a nano-indentation experiment.

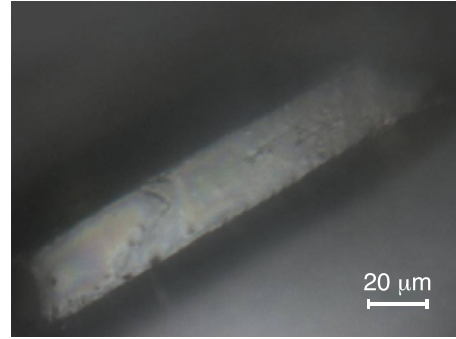


Figure S3: Optical microscope image of the measured MOF-74-Zn crystal.

ring stretching mode ν_{ring} , CH in-plane/out-of-plane bending modes $\beta(CH)_{ip}/\beta(CH)_{oop}$, and $\beta_{as}(COO)/\beta_s(COO)$ modes experience significant perturbations as shown in Fig. S4.

The assignment of the MOF phonon modes was carried out by comparison with the spectra of reported salicylate compounds (see Table S1).^{10,11} However, under 760 Torr CO_2 , the perturbations are negligible (see Fig. S4). The perturbations observed by IR spectra suggest stronger interactions of H_2O molecules with the MOF structure than CO_2 molecules, as attested by our first-principle calculations. The observation is consistent with previous X-ray diffraction results showing that water inclusion into the MOF-74-Zn and MOF-74-Co frameworks causes an elongation of the metal-oxygen bond distance.¹² The spectra of the activated and hydrated MOFs are shown in Fig. S5. The spectra of MOFs under 760 Torr CO_2 are shown in Fig. S6.

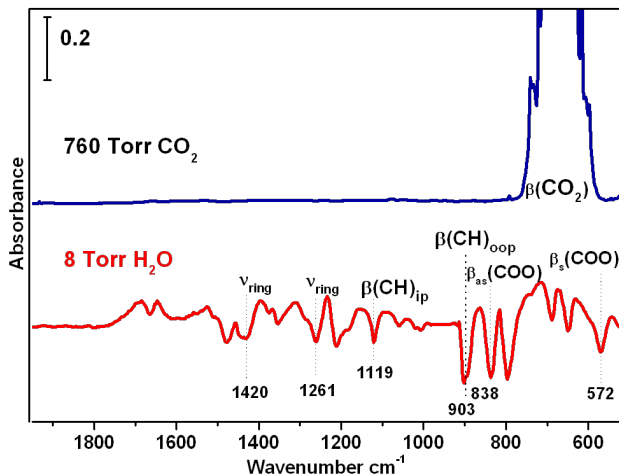


Figure S4: Difference spectra of MOF-74-Zn after adsorption of CO₂ (blue) under 760 Torr and H₂O (red) under 8 Torr, referenced to the activated MOF-74-Zn under vacuum. Note that the difference spectra highlight the shift of MOFs phonon modes, the original position MOFs' phonon modes is shown in Table S1 and Figs. S5, and S6.

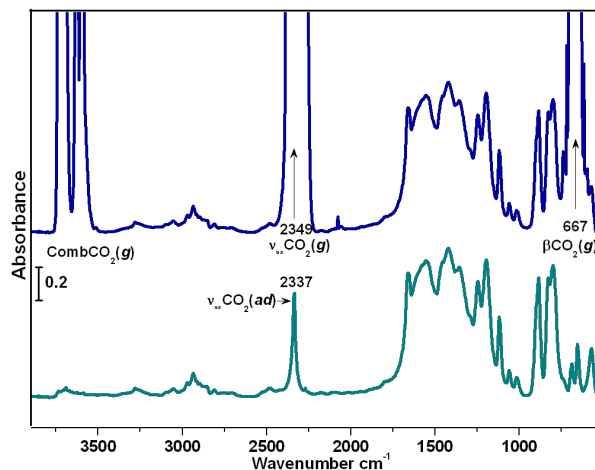


Figure S6: IR absorption spectra of activated MOF-74-Zn under 760 Torr CO₂ (blue) and after evacuation of gas phase CO₂ for 0.5 min (cyan). All the spectra reference to a KBr pellet in vacuum.

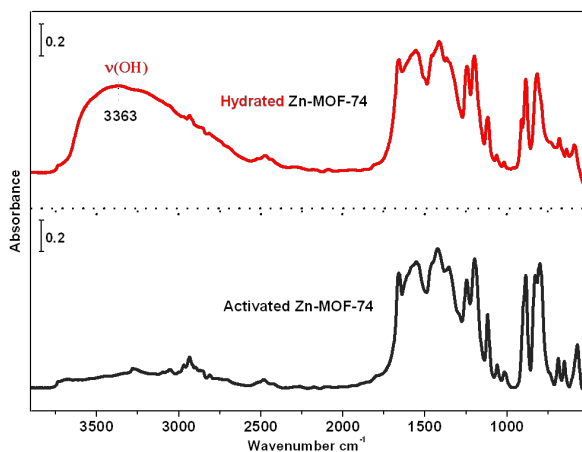


Figure S5: IR absorption spectra of activated (black) and hydrated MOF-74-Zn (red) by 8 Torr H₂O vapor. All the spectra reference to a KBr pellet in vacuum.

Table S1: Assignment of selected bands (in cm⁻¹) from infrared spectra of activated MOF-74-Zn. Numbers 19a, 14, 9b, and 17b represent Wilson notation to describe the phenyl vibrational modes.¹³

Freq.	Assignment	Wilson No.
1554	$\nu_{as}(\text{COO}^-)$	—
1458	$\nu(\text{CC})_{ar}$	19a
1422	$\nu(\text{CC})_{ar}$	14
1356	$\nu_s(\text{COO}^-)$	—
1247	$\nu(\text{CC})_{ar}$	—
1197	$\nu(\text{C-O})_{phenylic}$	—
1119	$\beta(\text{C-H})$	9b
902	$\beta(\text{C-H})$	17b
799,572	$\beta_{as}(\text{COO}^-)/\beta_s(\text{COO}^-)$	—

References

- (1) Ashcroft, N. W.; Mermin, N. D. *Solid State Physics*; Thomson Learning Inc., 1976.
- (2) Rappe, A. K.; Casewit, C. J.; Colwell, K. S.; Goddard III, W. A.; Skiff, W. M. UFF, a full periodic table force field for molecular mechanics and molecular dynamics simulations. *J. Am. Chem. Soc.* **1992**, *114*, 10024.
- (3) Gale, J. D. G. Empirical potential derivation for ionic materials. *Phil. Mag. B* **1996**, *73*, 3.
- (4) Gale, J. D. G. GULP: A computer program for the symmetry-adapted simulation of solids. *J. Chem. Soc., Faraday Trans.* **1997**, *93*, 629.
- (5) Gale, J. D. G.; Rohl, A. L. The General Utility Lattice Program. *Mol. Simul.* **2003**, *29*, 291.
- (6) Yazaydin, A. O.; Snurr, R. Q.; Park, T.-H.; Koh, K.; Liu, J.; Levan, M. D.; Benin, A.; Jakubczak, P.; Lanuza, M.; Galloway, D. B.; Low, J. J.; Willis, R. R. Screening of Metal-Organic Frameworks for Carbon Dioxide Capture from Flue Gas Using a Combined Experimental and Modeling Approach. *J. Am. Chem. Soc.* **2009**, *131*, 18198.
- (7) Simmons, G.; Wang, H. *Single Crystal Elastic Constants and Calculated Aggregate Properties*; MIT, Cambridge, MA, 1971.
- (8) Oliver, W. C.; Pharr, G. M. An improved technique for determining hardness and elastic modulus using load and displacement sensing indentation experiments. *J. Mater. Res.* **1992**, *7*, 1564–1583.
- (9) Lu, H.; Wang, B.; Ma, J.; Huang, G.; Viswanathan, H. In *Measurement of Creep Compliance of Solid Polymers by Nanoindentation*; Proulx, T., Ed.; Mechanics of Time-Dependent Materials; Springer, 2003; Vol. 7.
- (10) Humbert, B.; Alnot, M.; Quiles, F. Infrared and Raman spectroscopical studies of salicylic and salicylate derivatives in aqueous solution. *Spectrochim. Acta A* **1998**, *54*, 465.
- (11) Kalinowska, M.; Świslocka, R.; Borawska, M.; Piekut, J.; Lewandowski, W. Spectroscopic (FT-IR, FT-Raman, UV) and microbiological studies of disubstituted benzoates of alkali metals. *Spectrochim. Acta A* **2008**, *70*, 126.
- (12) Dietzel, P. D. C.; Johnsen, R. E.; Blom, R.; Fjellvåg, H. Structural Changes and Coordinatively Unsaturated Metal Atoms on Dehydration of Honeycomb Analogous Microporous Metal-Organic Frameworks. *Chem. Eur. J.* **2008**, *14*, 2389–2397.
- (13) Varsány, G.; Arkadévich, M.; Láng, K. L. *Assignments for Vibrational Spectra of 700 Benzene Derivatives*; Akadémiai Kiadó: Budapest, 1973.